CSIRO Publishing

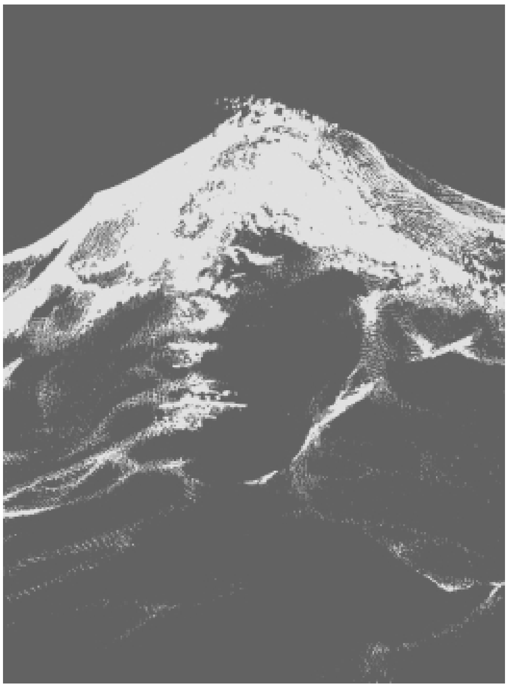

Marine & Freshwater Research

VOLUME 52, 2001

A journal for the publication of original contributions in physical oceanography, marine chemistry, marine and estuarine biology and limnology

All enquiries and manuscripts should be directed to:

Marine and Freshwater Research
CSIRO Publishing
PO Box 1139 (150 Oxford St)
Collingwood, Vic. 3066, Australia

Telephone: +61 3 9662 7618
Fax: +61 3 9662 7611
Email: mfr@publish.csiro.au

CSIRO PUBLISHING

Published by CSIRO Publishing
for CSIRO and the Australian Academy of Science

www.publish.csiro.au/journals/mfr

Mar. Freshwater Res., 2001, **52**, 475–89

Remote sensing of seabed types in the Australian South East Fishery; development and application of normal incident acoustic techniques and associated 'ground truthing'

R. J. Kloser, N. J. Bax, T. Ryan, A. Williams and B. A. Barker

CSIRO Marine Research, GPO Box 1538, Hobart, Tas. 7001, Australia. email: rudy.kloser@marine.csiro.au

Abstract. Calibrated acoustic backscattering measurements using 12, 38 and 120 kHz were collected over depths of 30–230 m, together with benthic epi- and in-fauna, sediments, photographs and video data. Each acoustic ping was envelope detected and digitized by echo sounder to include both the first and second echoes, and specifically designed software removed signal biases. A reference set of distinct habitat types at different depths was established, and a simple classification of the seabed combined both biological and geological attributes. Four seabed types were identified as having broad biological and geological significance; the simple acoustic indices could discriminate three of these at a single frequency. This demonstrates that the acoustic indices are not directly related to specific seabed properties but to a combination of seabed hardness and roughness attributes at a particular sampling frequency. The acoustic-derived maps have greater detail of seabed structure than previously described by sediment surveys and fishers' interpretation. The collection of calibrated digital acoustic data at multiple frequencies and the creation of reference seabed sites will ensure that new shape- and energy-based feature extraction methods on the ping-based data can begin to unravel the complexities of the seabed. The methods described can be transferred to higher-resolution swath-mapping acoustic-sampling devices such as digital side-scan sonars and multi-beam echo sounders.

Introduction

The present day seabed is a mix of recent biological, hydrological and chemical processes layered over a geological framework developed through the eons. Both the seabed and the invertebrate and fish communities are structured by depth, sediment types, latitude and hydrological processes (e.g. Snelgrove and Butman 1994; Coleman *et al*. 1997). However, the links between seabed landscape, or 'seascape', and animal communities are frequently not well described because of the difficulty of sampling broad areas of the seabed, especially over rough ground and at depth. In a recent study of the south-east Australian continental shelf, the relationships between animal communities and seabed type were established from point (or transect) samples by using a variety of fixed and mobile fishing gears, underwater photography and physical samplers (Bax and Williams 2000). Vertical sounding acoustics were used to determine where these samples should be taken and to provide maps of seabed types to generalize from point (or transect) samples to the broader shelf area. In this paper we describe the validation and results of that acoustic mapping.

Shape and energy features from the range corrected, enveloped acoustic signals obtained with normal incident high frequency narrow band acoustic systems have been used to characterize the seabed (Orlowski 1984; Chivers *et al*. 1990; Lurton and Pouliquen 1992; Collins *et al* 1996). Seabed descriptions have been based on simple analysis of both the first and second reflected echoes (Orlowski 1984; Chivers *et al.* 1990), or on detailed analysis of the first echo alone (Lurton and Pouliquen 1992; Collins *et al.* 1996). Fishers use similar features in their own seabed mapping. However, whereas it is clear that these descriptors provide relative information on the features (hardness and roughness) of adjacent seabed types at similar depths, or on particular prominent outcrops, it is not clear that these same descriptors can provide seabed descriptors that are consistent in different areas and over a wide range of depths (Bax *et al*. 1999).

The seabed of the south-east Australian shelf can be described using basic physical and biological properties such as soft, hard, rough and smooth seabed features. Using this approach, Bax *et al.* (1999) showed that relatively simple acoustic indices can produce biologically significant seabed characterization over a limited depth range, 40–60 m, although they noted a possible depth bias in the indices. This possible depth bias was a concern when extending the method to the depth range of the continental shelf in this area, 30–230 m. Previous researchers using commercial

10.1071/MF99181 1323-1650/01/040475

equipment — the RoxAnn system based on the classification scheme of Chivers *et al.* (1990) — to classify seabed type, have operated over narrow depth ranges (Magorrian *et al.* 1995; Kaiser *et al.* 1998) or found a possible depth bias (Greenstreet *et al.* 1997). Furthermore, data quality problems (Greenstreet *et al.* 1997) and biases due to varying ship speed (Magorrian *et al.* 1995) have been reported.

Clearly, we needed to establish the depth dependency in our data before we applied a general classification scheme over our wide depth range. Also, we needed to maintain data quality when trying to combine data recorded in a variety of sea states, from a number of surveys and with different instrument configurations. For these reasons we used a scientific echo-sounder that stores a digital record of the acoustic reflection from each acoustic ping. These raw data are re-analysed in this paper to determine the biases associated with sampling at different depths, and sea conditions. We apply simple energy-based feature extractions of the first and second seabed echoes following the techniques of Chivers *et al.* (1990). Extracted acoustic features are then compared with the ground-truth data obtained from a set of 10 reference seabed types that were also sampled with sediment grab, benthic dredge, photographic and video samplers. Finally, maps of the acoustic features are compared with sediment and fishers' interpretation maps of the region.

Material and methods

Study area

The study region was a section of the south-east coast of Australia between 36º and 39ºS (Fig. 1). In this region, the shelf extends to ~170–200 m depth and is 25 km wide in the north of the study region and over 175 km wide in the south. The seabed is a complex patchwork of massive sediment mosaics with limestone reefs, granite and sandstone bedrocks, and consolidated sediments outcropping in prominent tracts and dispersed patches (Bax and Williams 2000). In overview, the inner-shelf sediment plains of the western section are studded with patches of mostly low-relief limestones and sandstones, whereas to the east, smaller sediment plains are bounded mid-shelf by an elongated buttress of limestone patch reefs. In the eastern regions, sediment plains of the inner and outer shelf are bounded by the largest tract of hard-ground on the south-eastern shelf, the mosaic of limestone reefs forming the Gabo/Howe Reef complex. The shelf break is marked by structurally complex features formed by the necks of the Bass Canyon. Our sampling combined low intensity sampling over a broad area (as shown by the vessel tracks in Fig. 1) and intensive sampling targeted in areas of heterogeneous seabed (mesohabitats in Fig. 1).

Reference seabed types

We 'calibrated' or ground-truthed our interpretation of acoustic data by intensively sampling 10 reference sites with multi-frequency acoustics and physical samplers. A range of reference sites was selected that provided contrasts in seabed type and depth; these were situated within 'mesohabitat' study areas known to have heterogeneous substrata with a variety of associated epibenthic communities (Bax and Williams 2000). The data evaluated for each reference site included acoustic indices and echograms, seabed depth and position, photographic

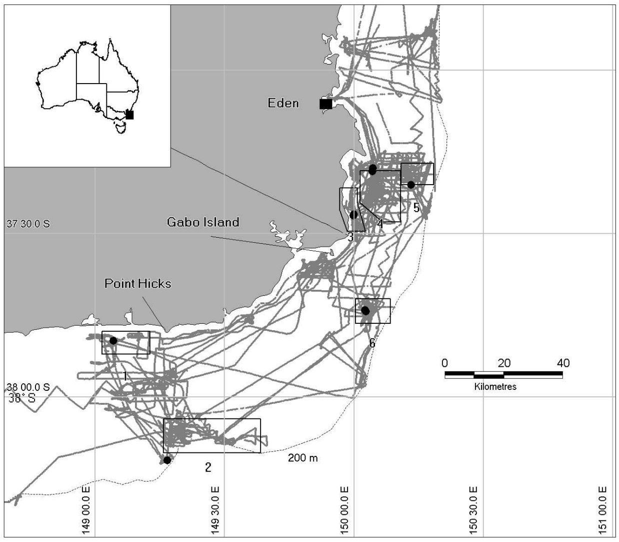

Fig. 1. Map of the South East Fishery (SEF) region for the ecosystem study, with mesohabitats and the vessel tracks where acoustic data were collected for voyages in April and December 1996. Mesohabitats (10s of metres to 1 km) are 1, Point Hicks; 2, Horseshoe; 3, Black Head; 4, Disaster Bay; 5, Big Gutter; 6, Gabo Reef. Reference sampling sites are highlighted with dots.

imagery, identification of sediment-type or lithology, and epibenthic community type (Table 1). A flow diagram of the data collection and processing from the various samplers is shown in Fig. 2.

Biological, physical and visual sampling

Invertebrate epifauna and infauna were collected with a large benthic dredge along transects of approximately 1200 m length (corresponding to a tow speed of ~1 m s^{-1} for 20 min). Our assessment of community type was based on these biological samples in conjuction with photographic images. We used two camera systems to provide image data: a 35 mm Photosea camera mounted on the benthic sled, and a video camera on a towed platform (Barker *et al.* 1999). The towed video platform was particularly useful over rough ground that could not be sampled by the sled. Images were taken at 12 s intervals (~12 m) during sled transects. Sediments were collected initially by a Smith McIntyre grab, but subsequently by a pipe dredge, and a collecting box situated on one skid of the benthic sled, because of the loss of the grab. The mean grain size for each sample was calculated by the method of moments (Folk 1968). Rock samples were collected opportunistically from the benthic sled and fishing gears and classified from slabs and thin-sections (Bax and Williams 2000).

Normal incident acoustics

Plate I shows the normal incident narrow conical beam sounding technique and the process of formulation of the first and second echo. The displayed echogram represents a recording of the returned echoes from repeated individual acoustic pulses. The acoustic waveform of the returned echo is band-passed and the squared echo is envelope detected. The recorded enveloped wave shape differs from the outgoing acoustic pulse because of the following factors:

(1) impedance mismatch between the seabed and seawater leading to surface scattering of the main pulse;

(1) acoustic instrument parameters such as transmitter power, frequency, pulse length, transducer beampattern, receiver bandwidth and pulse length;

Table 1. Qualitative attributes of reference seabed sites and a four-category classification based on reflectance properties (tail of first echo and energy in second echo)

Site no.	Depth (m)	Sediment type	Substratum appearance in a number of photographic frames or video associated to the echogram	Epibenthic community from the photographs supported by specimens retained in the sled	Viewing of echogram tail first echo	Viewing of echogram second echo	Acoustic seabed classification
a	55	Moderately sorted muddy sand	Flatly sloping	Intermittent low branching sponges/ mollusc beds	Low signal strength, short tail	Low signal strength	Soft-smooth
b	80	Unsorted muddy sand	Flatly sloping, unrippled	Sparse/intermediate irregular, bushy sponges; occasional bioturbation	Low signal strength, short tail	Low signal strength	Soft-smooth
c	34	Unsorted muddy sand	Flat, unrippled with scattered patches of consolidated substratum	Small bushy sponges in clumps	Medium signal strength, long tail	Low–medium signal strength	Soft-rough
d	37	Sorted coarse sand and shell fragments	Flat, regularly rippled (10–30 cm wavelength & amplitude)	Occasional mollusc beds; occasional bioturbation	Medium signal strength, long tail	Low–medium signal strength	Soft-rough
e	80	Unsorted muddy sand	Flatly sloping, unrippled sediment among scattered limestone slabs	Sparse/intermediate irregular, bushy sponges; occasional bioturbation	Low signal strength, short tail	High signal strength	Hard-smooth
f	125	Unsorted muddy sand	Flatly sloping, unrippled sediment adjacent to limestone reef	Occasional irregular bushy and branching sponges; occasional bioturbation	Low signal strength, short tail	High signal strength	Hard-smooth
g	125	Unsorted muddy sand	Flatly sloping, unrippled sediment adjacent to limestone reef	Sparse ascidians/sea pens; evidence of bioturbation	Low signal strength, short tail	High signal strength	Hard-smooth
h	52	Fossiliferous limestone reef	Slabs with crevices and ledges; small (<3 m) pinnacles, walls	Dense gardens of encrusting and erect (cup/finger) sponges, seawhips	Medium–high signal strength, long tail	Medium–high signal strength	Hard-rough
i	115	Fossiliferous limestone reef with layer of sediment	Reef margin: steep (45–90º), high-relief walls (>3 m) with ledges, overhangs, caves, alternating with sloping broken edge and boulders	Dense sponge gardens with occasional large cup sponges, prostrate plate sponges and highly branched finger sponges	Medium–high signal strength, long tail	Medium–high signal strength	Hard-rough
j	125	Fossiliferous limestone reef with layer of sediment	Reef platform: irregular undulations, hummocks; occasional small pinnacles (0.5–1 m) and undercut slabs (~1 sq m)	Intermediate/dense gardens of finger and cup sponges; occasional pancake urchins	Medium–high signal strength, long tail	Medium–high signal strength	Hard-rough

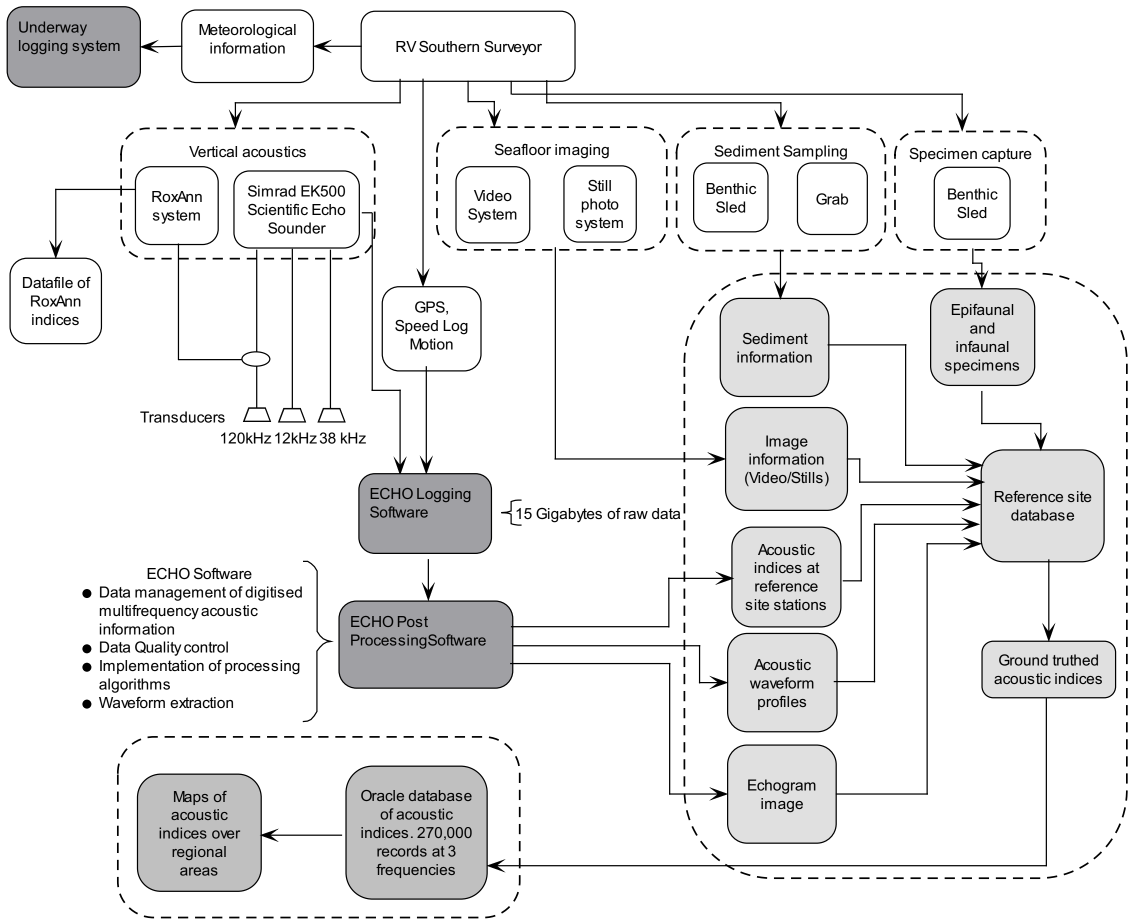

Fig. 2. Flow diagram of the data collection and processing system used to classify seabed types by combining information from acoustic, video, still photographs, sediment and benthic sled samples.

(1) penetration of the acoustic signal into the seabed leading to volume scattering of the main pulse;

(1) directional reflections at the seawater/seabed interface due to seabed roughness;

(1) time delay of off-axis echoes due to spherical spreading with changing depth;

(1) scattering response from the sea surface, vessel hull and subsurface bubbles for the second return echo;

(1) slope of the seabed and stability and trim of the acoustic platform;

(1) attenuation of the signal through the water column; and

(1) acoustic noise on the outgoing and returning signals.

Explicit models that represent the change in acoustic waveform due to this complex scattering and absorption mechanisms in four dimensions do not exist (but see Jackson *et al.* 1986). Simplified models have been developed to extract energy based indices of the seabed in terms of acoustic roughness and hardness (Orlowski 1984; Heald and Pace 1996) and we have used these in the analysis of the collected acoustic data.

Acoustic instrumentation. Acoustic seabed surveys were conducted from the 65 m RV *Southern Surveyor* with a Simrad EK500 echosounder. This echo sounder has a large (160 dB re 1 µPa) instantaneous dynamic range and digitizes the envelope-detected seabed signals from the peak bottom signals (20 dB re 1 µPa) down to sea state or instrument noise (–100 dB re 1 µPa), depending on frequency. The echo sounder was connected to three hull-mounted transducers operating at 12, 38 and 120 kHz. An additional 38 kHz transducer was mounted on a pole that could be lowered 3.5 m below the hull of the vessel in rough weather. The acoustic system was calibrated with a 42 mm tungsten carbide calibration sphere (Foote 1982; SIMRAD software version 5.3). This volume reverberation calibration technique combines the electrical and acoustic constants of the system, G_o^2 (for a given transmitter power, Pt, pulse length, τ, and band width) and the equivalent beamwidth, ψ (provided by the transducer manufacturer). Sound velocity, *c*, and absorption constant, α, are required to give range, *r*, independent values of the volume reverberation signal, Sv dB re 1 µPa at 1m, that is expressed in logarithmic form as:

$$10\log(sv) = 10\log(P_r) + 10\log(r^2 10^{2\alpha r}) - 10\log\left(\frac{P_t G_0^2 r_0^2 \lambda^2 c \tau \psi}{32\pi^2}\right) \quad \text{dB re 1 mPa at 1m.} \quad (1)$$

The 38 and 120 kHz transducers were split-beam transducers and the 12 kHz transducer was a single beam. One of the beams on the 120 kHz transducer was connected to a RoxAnn seabed instrument set up

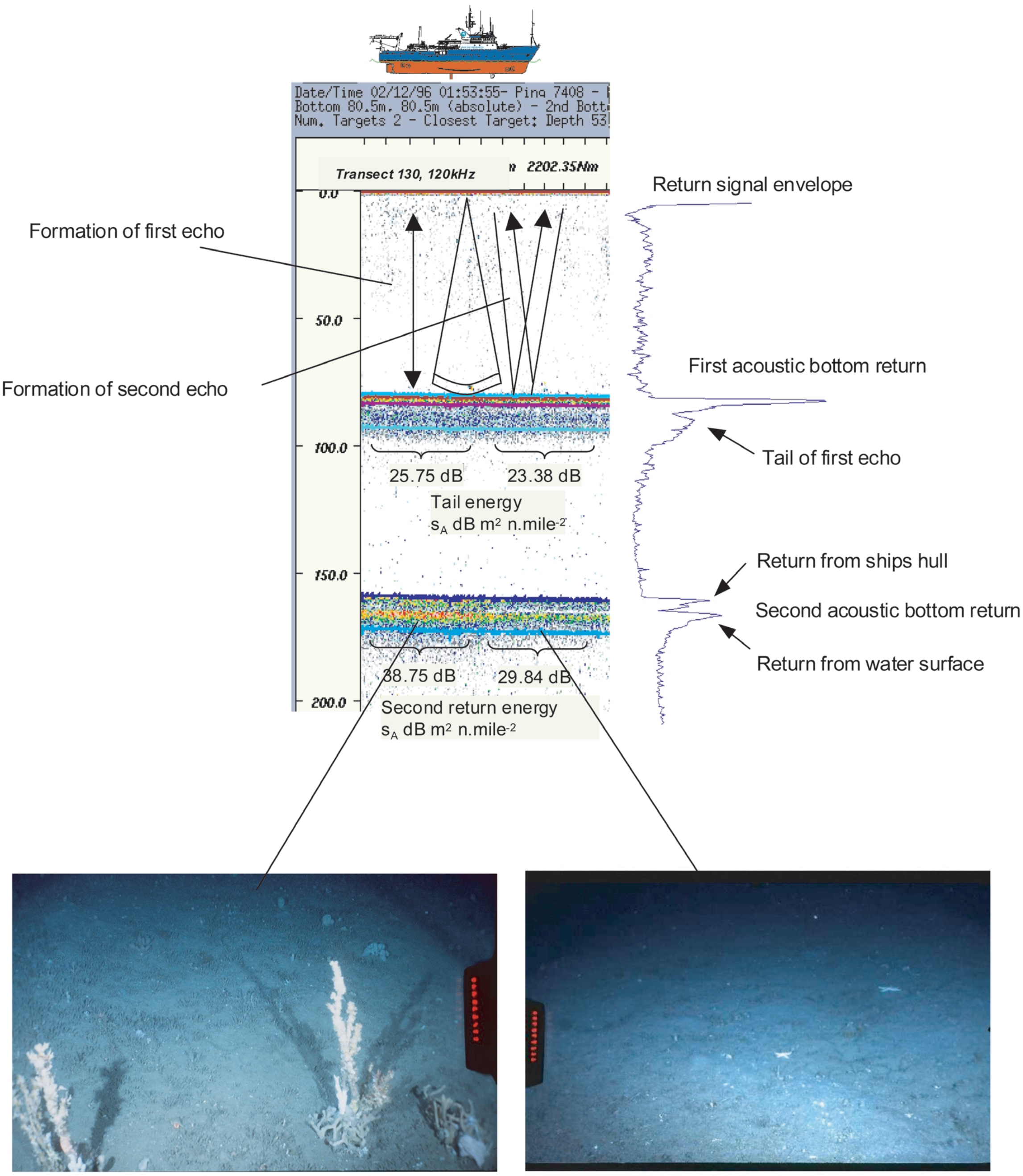

Plate I. Example echogram from the 120 kHz transducer showing the production of the first and second seabed echoes and associated water column scatter as logged by the ECHO software during a benthic sled tow. The echogram and associated still photographs show the transition from hard ground to soft ground and the associated change in benthic fauna. The change in acoustic hardness of the seabed is interpreted from the signal strength of the second echo. The values for acoustic roughness and hardness for the two seabed types are shown in dB.

according to manufacturer's instructions. Details of the acoustic calibration constants for all three transducers are given in Table 2.

Acoustic data collection. Acoustic volume reverberation (Sv) data were logged continuously from three frequencies using a software package, 'ECHO' (Waring *et al*. 1994; Kloser *et al*. 1998). The vessel's pitch/roll (at bottom detection), GPS navigation, speed and the digitized ping Sv dB re 1 µPa data from each frequency were logged. The Sv values from the Simrad EK500 were range-corrected and binned into depth cells. In the May 1996 survey, the three frequencies were digitized in 0.3 m depth cells. This did not provide optimal resolution of the first echo, so in the December 1996 survey the first and second echoes were averaged into either 0.5 m or 1 m bins as well as obtaining high-resolution first bottom echo data in 0.01 m bins. The high resolution first bottom echo was binned at a value greater than twice the pulse length assuring that the Nyquist sampling criterion was

Table 2. Calibration settings for the acoustic instrument

	Frequency			
	12 kHz	38 kHz	120 kHz	38 kHz Pole
Absorption (dB/km)	1	9	43	9
Pulse length (mS)	3	1	1	1
Bandwidth (kHz)	1.2	3.8	1.2	3.8
Calibration constant (Svc)	13.3	27.2	22.7	26.5
Beamwidth (between -3dB points) (degrees)	16/17.5	7.1	11.2	7.3
Equivalent beam width (dB re 1 steradian)	–13	–20.7	–18.5	–20.7

satisfied. Data from the RoxAnn instrument, that summarize limited data energy-based features from many pings, were collected in May 1996 for later comparison with digital data from individual pings. All data were logged on a personal computer integrated with the vessel's GPS. Overall there were 8 weeks of survey time, in which 15 GBytes of acoustic data were collected and archived.

Acoustic data quality (ECHO software). Archived digital bottom data were quality checked by using the ECHO post-processing software to mask out bad data as indicated by obvious signal attenuation, usually because of strong winds and/or sea-state. This signal attenuation could be observed on the echograms by examining the loss of water column acoustic scatter as well as seabed acoustic tail scatter relative to adjacent records. Bad weather produced pronounced aeration under the vessel's hull, resulting in increased acoustic reverberation close to the transducer and a marked attenuation of the tail of the first echo and the whole second echo. When sea conditions were particularly poor, a whole day's data would be lost because of poor acoustic signals. In contrast, the RoxAnn instrument, which was receiving the same poor acoustic signals, continued to classify and record seabed type, with no reference to the low quality of these classifications.

Acoustic data analysis. Simple indices of seabed roughness and hardness were derived from the acoustic data, by integrating the tail of the first echo and all of the first and second seabed echoes (Orlowski 1984; Chivers *et al.*1990; Heald and Pace 1996). The reflected acoustic energy in the tail of the first echo, that is increasingly scattered on a rougher seabed, represents acoustic seabed roughness. Several algorithms were used to implement this in our 'ECHO' software. First, a constant depth algorithm was used to integrate the tail echo from 5 to 20 m below the detected bottom signal. This index was found to increase linearly with depth because of spherical spreading of the beam lengthening the return signal envelopes. To compensate for this lengthening, a second tail echo algorithm was implemented that integrated a constant angular sector of the seabed echo off axis from the normal incident beam (Heald and Pace 1996). The limit on the start angle was based on the pulse length and the minimum water depth. For our depth range and 1 mS pulse lengths, the tail portion of the first echo was integrated between depth intervals, di, as determined by the bottom depth and off-axis angular values, θi, between 20° and 30° referenced to the start of the bottom echo. The pulse length offset was set at 0 and 1.5 m, where:

$$\mathrm{d}i = bottom\_depth*\left(\frac{1}{Cos\theta i}-1\right) + pulse\_offset.$$

The entire reflected energy in the second echo, that has been reflected from the seabed twice (seabed–ship and sea water surface–seabed–ship), represents acoustic hardness. It was defined as starting at two times the water depth (d1) and ending at two times water depth plus 30 m (d2). Several pings, p, were integrated (20–60 depending on vessel speed of 3–10 kn) to reduce between-ping variability in the backscatter returns and to standardize on a unit of length sampled, 92.6 m (0.05 nmile):

$$\bar{S}_A = 10\log_{10}\left(1852^2 4\pi \frac{\sum_{p=1}^{m}\left(\delta d \sum_{d=d1}^{d2} 10^{\frac{sv_{dp}}{10}}\right)}{m}\right) \text{dB re m}^2\ \text{nmile}^{-2} \qquad (2)$$

where S_A is the area backscatter coefficient, integrated between the start, $d1$, and stop, $d2$, depth, and δd is the acoustic sampling interval. The derivation of area backscatter stems from fishery acoustic biomass studies and is used here as a relative measure of acoustic energy for volume scattering (SIMRAD 1996).

Reflected acoustic waveforms collected at the 10 reference sites were extracted and compared with physical samples at various depths. In order to compare the echo tail energy and shape at different depths, the signals were transformed to a reference depth of 100 m. The tail echos (defined as commencing after a delay of the pulse length in water) were resampled at an effective rate of the ratio of the water depth to the reference depth.

Results

RoxAnn acoustic analysis

Acoustic seabed classifications obtained with the RoxAnn system on the 120 kHz transducer contained major depth biases (Fig. 3). The depth bias in these data (393 407 points collected over a four-week survey) could not be explained by differences in bottom type as determined from sediment and photographic samples. Both the roughness and hardness indices reached a maximum and were then clipped at 130 and 70 m, respectively. The depth trend prior to data clipping could be removed by carefully extracting data from calm days, and the resulting data compared favourably with data from our own algorithms, and field-based sampling with photographic, video and sediment samples. Data beyond 70 m for the hardness parameter could not be recovered and we discontinued use of the data set.

Digital acoustic data analysis

The digital data were calibrated, quality assured and processed as outlined in the methods, with scatter plots of the indices produced to observe trends with depth and frequency. The 120 kHz frequency data appeared to need no overall depth correction for any of the extracted indices. A slight trend in the constant angle algorithm was observed in shallow water, <50 m. This was caused by an error in our

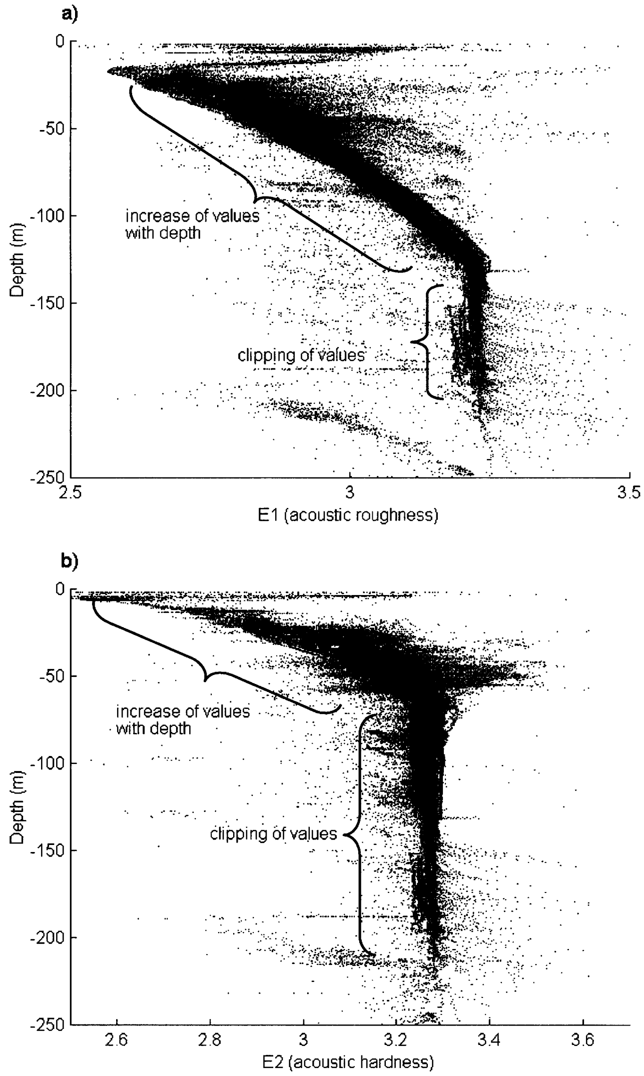

Fig. 3. Scatter plot of RoxAnn indices, E1 (roughness) and E2 (hardness), with depth collected during a four-week voyage. The indices show a clear depth bias and once clipped could not be recovered. Use of these data was discontinued due to this bias and uncertain data quality.

algorithm and was corrected by introducing a pulse offset of 1.5 m. A much greater depth bias occurred with the 38kHz data, Fig. 4(*a*), which was also corrected by introducing a pulse offset of 1.5 m. Figure 4(*b*) shows the uncorrected energy of the first echo tail that required a linear correction of –0.08 dB m^{-1}, Fig. 4(*d*). The total second echo energy for the 38 kHz frequency needed no obvious depth correction, Fig. 4(*c*).

Surficial sediment data

Mean sediment grain size is plotted against the derived acoustic indices and depth for one frequency 120 kHz (Fig. 5 *a*–*c*). There is a slight correlation between the hardness and roughness parameters and phi size (Figs 5*b* and 5*c*). This correlation occurred for all frequencies —12, 38 and 120 kHz — with r^2 of 0.3, 0.3 and 0.5 for acoustic hardness and 0.1, 0.2 and 0.3 for acoustic roughness, respectively. The plot of the residuals shows a random relationship for all frequencies and both indices. We did not observe a depth-related bias in the sediment size for depths less than 170 m, Fig. 5*a* (r^2 = 0.03) and there was no trend in the residuals that we could ascertain from the data collected. Sediment samples at depths greater than 170 m were not included in the linear model as they appear to contain larger grain sizes when compared with previous studies (Bax and Williams 2000). This suggests that some winnowing may have occurred in our sediment samples from greater depths.

Reference sites

The 10 reference sites were characterized by depth, sediment type, substratum appearance and epibenthic community (Table 1). Based on the characteristics of the first and second echoes, the 10 sites were divided into 4 seabed types: soft-smooth; soft-rough; hard-smooth; and hard-rough. Acoustic hardness and roughness indices for both the 38 and 120 kHz were plotted against these seabed types.

There is general agreement between seabed types, confirmed with physical and photographic sampling, and the acoustic roughness and acoustic hardness indices (Fig. 6). There are obvious outliers, for both soft-rough (reference Site *d*; Plate II*d*) and hard-rough (reference Site *h*; Plate II*h*) seabed types. Photographs show that these stations represent the extreme of our simple classification system. Reference Site *d* was a coarse sand sediment (phi 0.2), with large (10–30 cm) wavelength and large (10–30 cm) amplitude sand/shell regular wave patterns (Plate II*d*). The acoustic indices for this seabed were hard because of the coarse sediment and shell debris and very rough because of the sand waves.

The difficulty in characterizing the soft-rough seabed feature is highlighted by observing the average first echo tail waveforms of the four different seabed types referenced to 100 m at 38 and 120 kHz (Fig. 7*a* and *b*). The soft-rough seabed type is distinct at 38 kHz, but merges with the hard-smooth seabed type at 120 kHz, showing the dependence of seabed classification on acoustic frequency.

Reference site *h* (Plate II*h*) was a very rough hard reef with large boulders of 2–3 m vertical extent and massive branching epibenthos that represents the extreme of the rough-hard seabed types. There was a marked difference in the roughness index for this site for the two frequencies, which again highlights the frequency dependence of seabed typing by using acoustic systems.

Discussion

One of the important observations that has come from this work is the difficulty of remote sampling the seabed for biological and geological information in the open ocean.

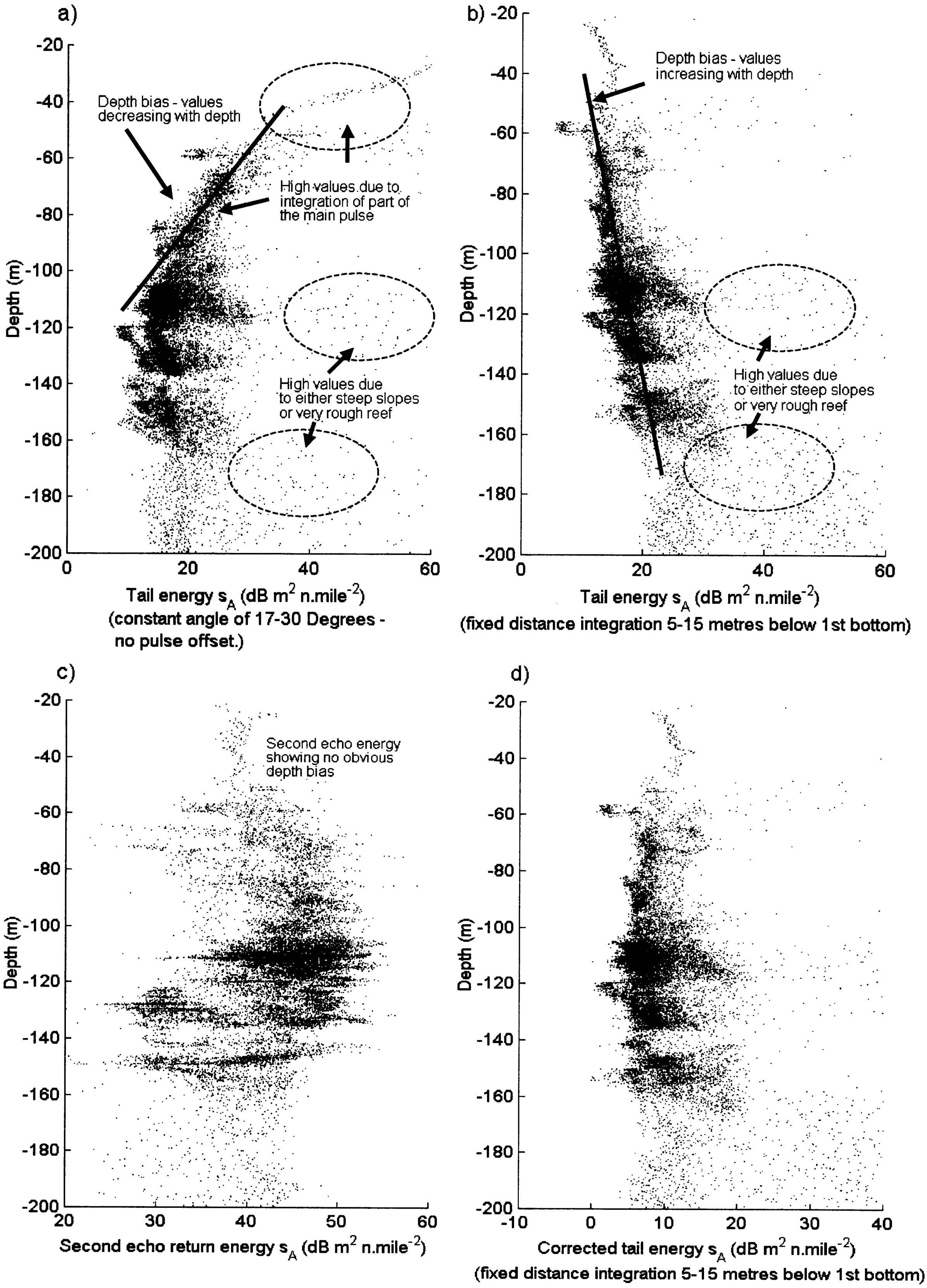

Fig. 4. Scatter plot of 40000 uncorrected acoustic indices: *(a)* tail of first echo constant depth, 38 kHz with depth bias at shallow depths due to integration close to the high-energy surface scattered echo; *(b)* tail of first echo constant angle, with depth bias due to time spreading, 38 kHz; *(c)* energy of second echo with no obvious depth bias, 38 kHz; and *(d)* tail of first echo, 38 kHz with depth bias removed.

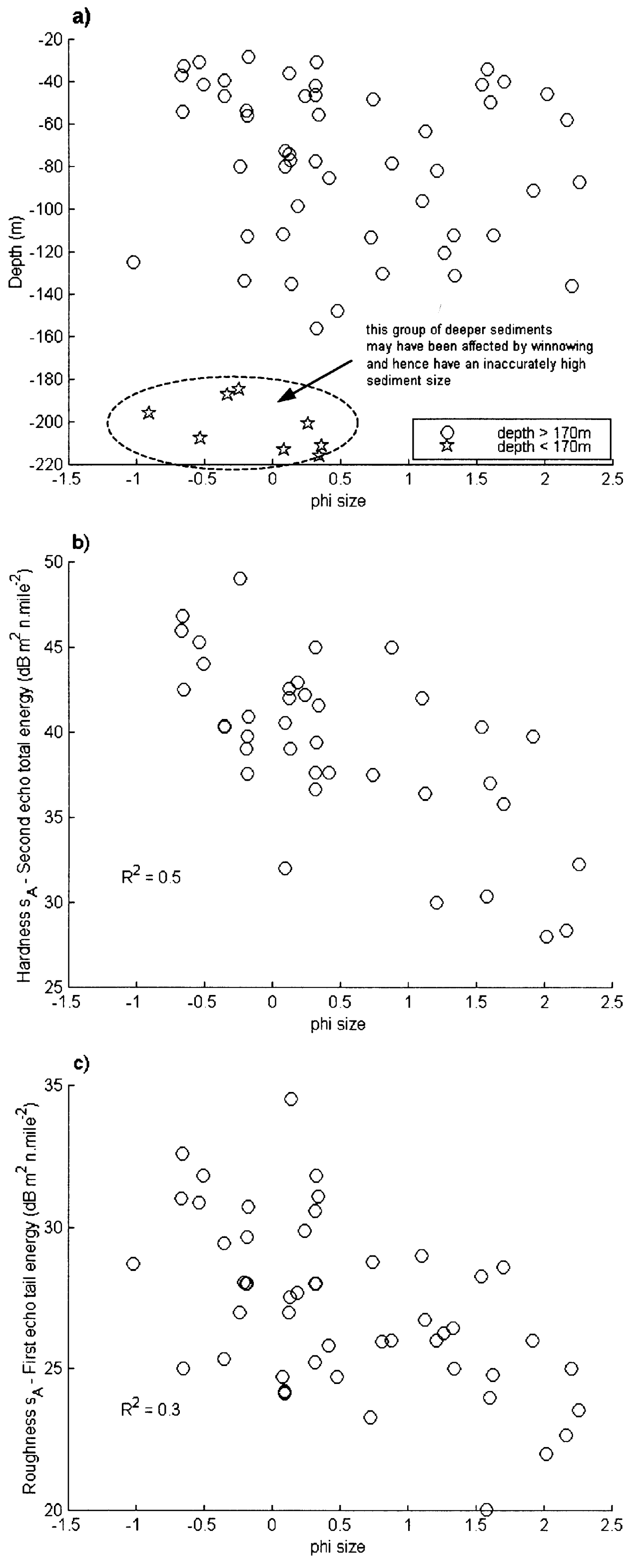

Fig. 5. Scatter plot of mean sediment phi size against depth, acoustic hardness, acoustic roughness and associated goodness-of-fit to a linear model. Samples collected from deeper than 170 m have been removed because of suspected winnowing of smaller sediments.

This was due to the various sea states we encountered, which at times reached 40–50 knot winds and 4–5 m seas. Maintaining data quality of our hull-mounted acoustic system was difficult and required that we log the digital data and use rigorous post-survey quality control. The ECHO software was used to exclude regions of bad data from the analysis (Kloser *et al.*1998). This interactive software enables the user to make changes in colour map, dynamic range, calibration, noise and bottom algorithms. The results of changes can then be directly observed in a 'what you see is what you get' (wysiwyg) software environment. This level of quality control resulted in rejecting entire days of data collected on particularly rough days. In contrast, the commercial instrument operating at the same time continued to classify and record seabed types with no notation that the data were of very poor quality and classifications were based primarily on acoustic interference.

Overall, our use of the commercial seabed system did not yield repeatable results and could not be used at depths greater than 70 m. Such devices cannot be relied on for repeatable measurements in the variety of sea and background noise conditions that we operate under. Others have experienced problems with this system and advocate the use of constant speed because of sensitivities to noise and/or subsurface bubbles (Hamilton *et al.* 1999). On the other hand, other researchers have obtained good results with the instrument (Magorrian *et al.* 1995; Greenstreet *et al.* 1997), although biases due to depth or ship speed were noted by both researchers.

A second major advantage of archiving calibrated digitized waveforms for subsequent quality control (instead of summary descriptors) is that the original data are available for subsequent analyses. Seabed typing is in its infancy and will only proceed through exploratory analyses of calibrated digital data collected from well described reference sites. We are now at the stage where we can introduce new algorithms (energy and shape based) that can describe more of the variability in seabed type than the simpler indices available at present. These can then be tested against our present reference sites and against future reference sites in different regions or collected from different platforms because all acoustic data are calibrated and digitized.

An alternative platform for acoustic sampling is the commercial fishing vessels. Fishers make extensive use of echo-sounders for targeting seabed type based on their interpretation of the acoustic returns and deployment (successful or not) of fishing gears (Bax and Williams 2001). Their interpretation of echo sounding is similar to the quantitative energy descriptors described by Orlowski (1984) and Heald and Pace (1996), and this raises the possibility that echo-sounders on fishers' vessels could be used to collect acoustic data and map the seabed during their routine operations. If we could calibrate and record acoustic

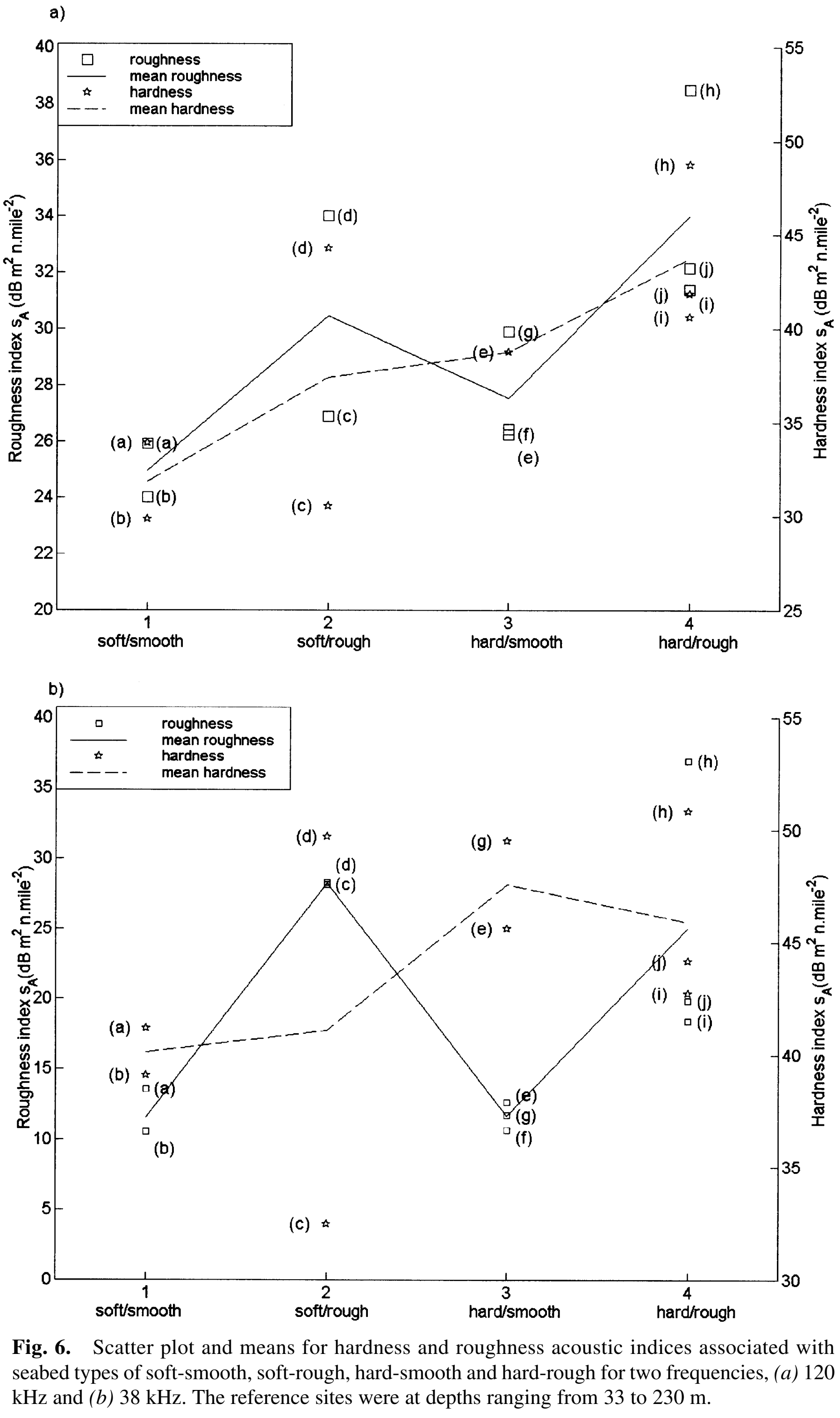

Fig. 6. Scatter plot and means for hardness and roughness acoustic indices associated with seabed types of soft-smooth, soft-rough, hard-smooth and hard-rough for two frequencies, *(a)* 120 kHz and *(b)* 38 kHz. The reference sites were at depths ranging from 33 to 230 m.

data collected by the fishing industry it would enable large areas of the shelf seabed to be mapped, without the high costs of a dedicated survey.

One of the issues that we foresaw in using acoustics over a relatively large depth range (30–230 m) was a depth bias. A depth-related bias occurs (at least in part) due to the greater sampling area with increasing depth because of spherical spreading of the beam. The physical mechanism for this process has been described and corrections attempted. In particular, Orlowski (1984) measured a depth

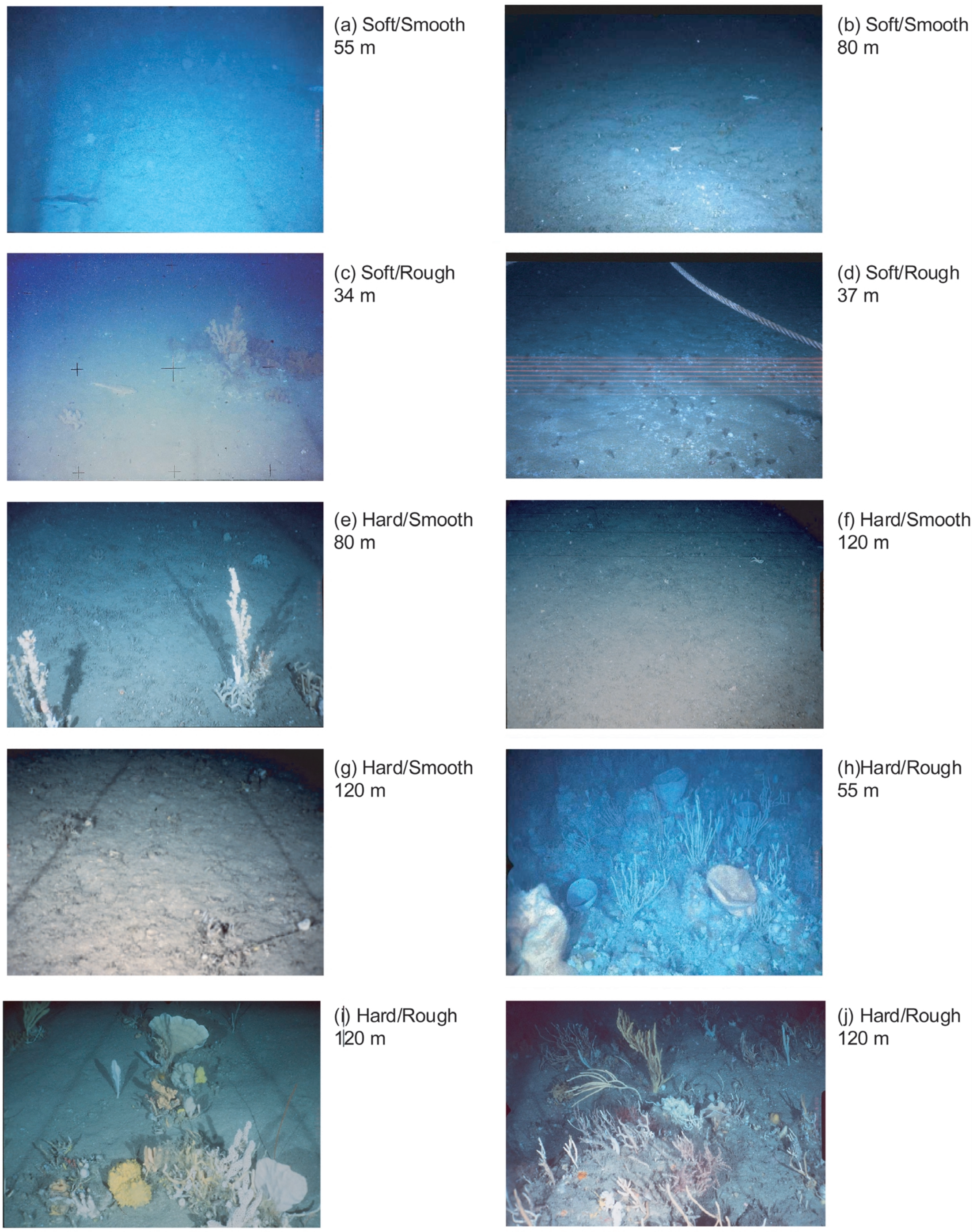

Plate II. Seabed images from the 10 reference sites *a–j* corresponding to the classifier descriptions outlined in Table 2. (Tow bridle of camera platform visible in most photographs.)

dependency when studying the reflection from the first and second seabed echoes, finding the results from depths less than 50 m to be unexplainable. From our scatter plots (Fig. 4) of the acoustic indices we did not appear to have an obvious depth-related bias for the acoustic roughness and hardness parameters. The constant depth roughness algorithm does have a depth bias for 38 kHz, but after linear model correction, compares well with the constant angle algorithm for the latter part of the depth range. The 120 kHz system did not appear to have a depth-related bias perhaps because of the wider beam width (10º) of this transducer. This result suggests that a wider beam width system is more

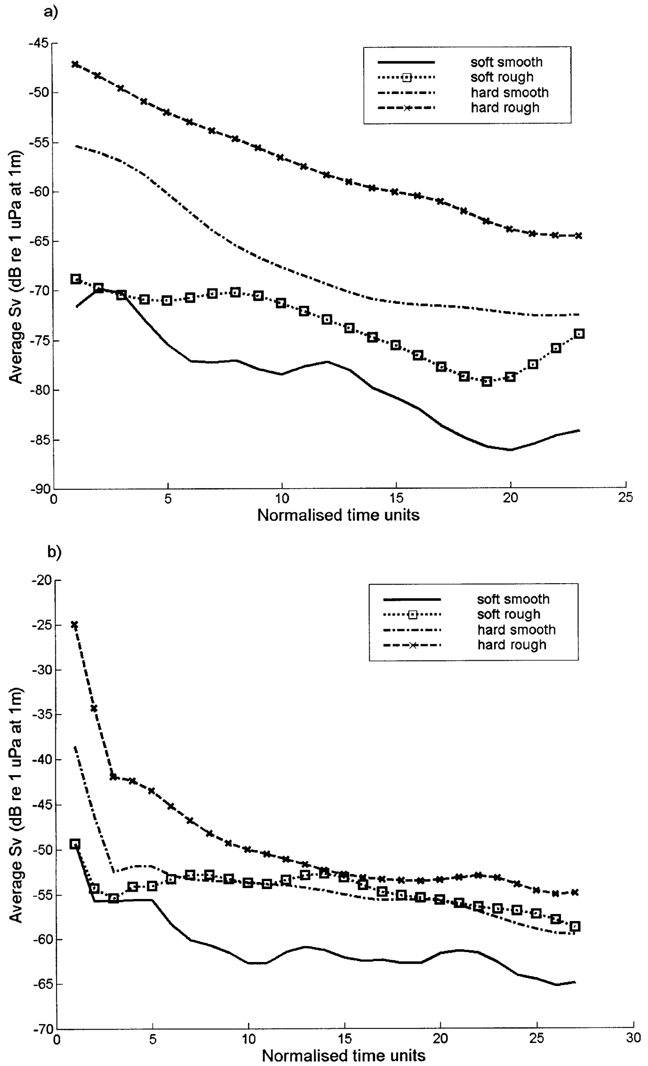

Fig. 7. Waveforms of the averaged seabed echoes for reference habitat types of soft-smooth, soft-rough, hard-smooth and hard-rough after compensation for depth at *(a)* 38 kHz and *(b)* 120 kHz.

suitable for obtaining these types of bottom roughness scatter measurements. This is consistent with improved discrimination of bottom scattering strength as a function of sediment size with increased angles of incidence (Urick 1983, p. 277).

Slope of the seabed introduced a bias that was difficult to exclude without a knowledge of the underlying bathymetry. Steep slopes produced large acoustic roughness values and low acoustic hardness values. If the vessel was transecting normal to the slope, these values could be flagged, but if the vessel was steaming parallel to the slope contours the values could only be interpreted once the data were plotted on a bathymetric map of the region. On very steep slopes such as drop offs from reefs, the large roughness parameter is indicative of a unique biological community and would be important to leave in the data set. This type of information could be excluded in data cleaning procedures used currently for the RoxAnn system (Greenstreet *et al.* 1997; Hamilton *et al.* 1999). Hence a seabed that produced a very high acoustic roughness and a very low acoustic hardness was indicative of sloping ground. The narrow-beam 38 kHz transducer seemed to be more sensitive to seabed slope than the wider beam 120 kHz system.

One of the tests for the acoustic hardness index was its ability to discriminate sediment grain size over a range of depths. Although the relationship is relatively weak — grain size explained 50% of variability in the hardness index for the 120 kHz system — it is a surprisingly good result given the simplicity of this acoustic index that measures only the total acoustic backscattering energy in the second bottom echo. The theory of the scattering mechanisms that make up the second echo is poorly understood (but see Heald and Pace 1996) and the effect that changing surface roughness, subsurface aeration (wind or propeller cavitation) and different hull shapes has not been quantified. Similarly, the backscatter from the same hull shape for changing pitch and roll angles is also open to question. Finally, sediment size is only one of many factors that constitute acoustic backscattering; sediment porosity, bulk density and surface roughness are also major contributors (Urick 1983).

The suitability of the second echo as a proxy for sediment size, or more correctly sediment hardness, is a significant step. Physical sediment surveys are expensive and consequently either cover a small area or a larger area at low resolution. Sediment sampling on the south-east Australian shelf has been performed by very sparse sampling with transects spaced every 20 Nm and stations every 10 nmile across the shelf (Davies 1979; Jones and Davies 1983). With acoustic methods, we are observing inferred changes in sediment properties at the scale of 0.5 nmile during continuous steaming at 8 kn or more, depending on sea state. However, acoustic sampling itself is at present insufficient to describe sediment properties without concomitant ground-truthing. Combining surficial sediment sampling with the acoustic hardness index provides a realistic option to improve the sediment maps of this region (Plate III*b*).

The reference seabed set established for ground-truthing in this study incorporated acoustic, video, photographic and benthic sampling. Our simple description of four seabed types based on a combination of biological and geological attributes is evolutionary (Bax *et al.* 1999). Therefore, we were encouraged by the consistency across depths for the soft-smooth, hard-smooth and hard-rough seabed types and their correct acoustic classification. Of interest was the anomalous soft-rough classification, where sand waves of coarse grain were classified as hard-rough by using the simple acoustic indices. There can obviously be a mismatch between acoustic-determined seabed types determined from

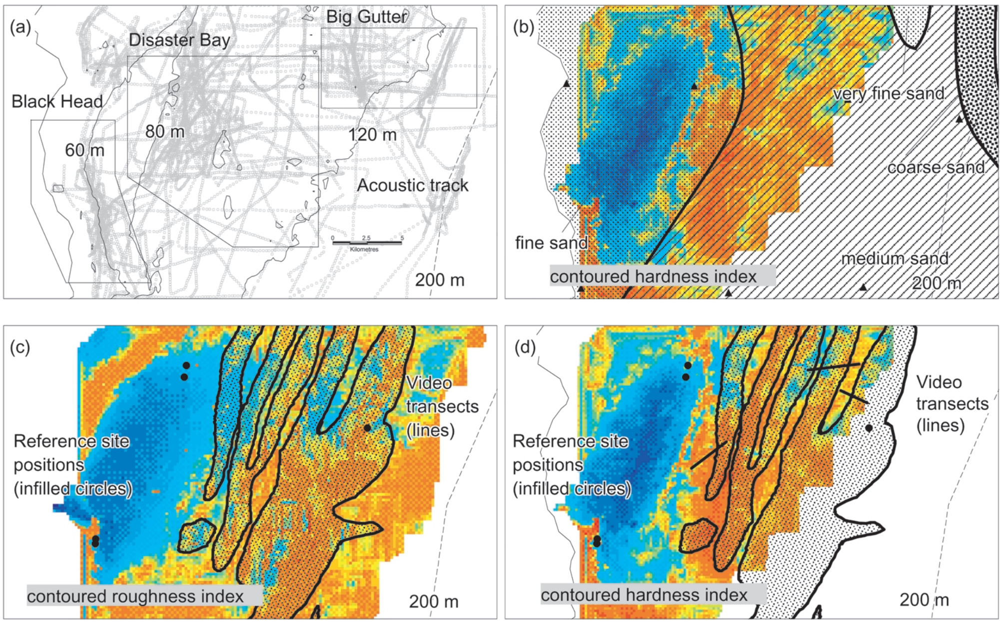

Plate III. Maps of acoustic hardness and roughness indices (120 kHz) compared with other maps of the region: *(a)* bathymetry with acoustic transects and habitat regions overlaid; *(b)* acoustic hardness with sediment maps from Davies (1979); *(c)* acoustic roughness with fishers' map of untrawlable ground map (Bax and Williams 2001); and *(d)* acoustic hardness with fishers' map of untrawlable ground map. Blue represents a low index value and orange a high value. Video transects used to study fine scale differences in the fishers' and acoustic maps are highlighted with dark lines.

these simple acoustic indices and seabed types determined from physical sampling and *in situ* visual examination. The importance of *in situ* visual examination as well as sediment sampling is suggested by the Greenstreet *et al.* (1997) review of RoxAnn. These authors found that six or seven seabed types were distinguished acoustically, but sediment sampling could confirm only three types. Sediment sampling would not have picked up features such as sand waves and it remains unclear whether the RoxAnn or the physical sediment samples provide a more realistic representation of the seabed in their area.

To compare our maps with those of previous studies on seabed character in this region we mapped the acoustic indices for the intensely sampled meso-habitats (Big Gutter, Disaster Bay and Black Head), using Vertical Mapper in Mapinfo (rectangular interpolation, cell size 0.005 deg., search radius 0.01 deg.). These maps are overlaid with bathymetry (Plate III*a*), and fishers' interpretation of seabed type (Plate III*c* and *d*). There is general agreement between the maps at large scale >10 km but not at fine scale <1 km (Williams and Bax 2001). The fine scale resolution of the acoustic maps highlights differences in interpretation between acoustic maps and fishers' maps at this single frequency. Detailed video sampling stations (159, 190 and 195, Plate III*c* and *d*) at transition points in these maps support the acoustic interpretation of acoustic hardness and roughness for biological and seabed attributes as defined in our reference set (Table 2), suggesting that the fishers' seabed classification scheme is not consistent with our own. This is perhaps not surprising given that the two classification schemes have been developed for different purposes.

In this study we collected information from three frequencies, each of which has proven useful for seabed classification purposes. The 120 kHz, wavelength 1.25 cm system proved to be the most sensitive to noise because of the large absorption of the signal with depth. It provided the best visual discrimination in shallow water and this may be due to its wider beamwidth (Bax *et al.* 1999). It also seemed the most responsive to sediment size with a correlation coefficient of 0.5. The 38 kHz, wavelength 3.95 cm, system was the best mid-depth system (100–250 m), as the noise of the vessel did not effect the second echo. In rough weather we were able to lower a 38 kHz transducer 3.5 m below the hull and greatly reduce surface bubble attenuation problems. Hence, this system could operate in far more severe weather conditions. The usefulness of the 12 kHz system was not fully explored in this analysis because of its poor discrimination of surficial sediment data.

Combined use of all three frequencies for classification of seabed types is part of ongoing research. Initial results of combining all three frequencies with energy and shape based features of the echo show great promise (Kavli *et al.* 1994; Kloser *et al.* 1998; Pitcher *et al.* 1999). The promise of multifrequency techniques is suggested by the large variability in the simple roughness and hardness indices observed with the 38 and 120 kHz frequencies, implying that the different frequencies (or potentially different beam widths) obtained different information (or the same information at different scales) from seabed features. More detailed classification and signal extraction methods on a larger number of frequencies may be able to classify a larger number of seabed types with greater consistency. However, we stress again that this will only be possible by using calibrated acoustic data in their raw form, collected from reference areas that have been ground-truthed.

Looking to the future, we will expand our limited reference set to form a comprehensive reference set of seabed descriptors. To date, we have used only simple, vertical single-beam acoustic systems. However, the advantage of the methodology described here is that it can be applied to calibrated acoustic data collected from a broad range of sampling platforms from fishing vessels to multi-frequency, split beam scientific sounders or even higher resolution swath mapping acoustic systems such as digital sidescan sonars and multibeam echo sounders. This will enable more detailed and more consistent seabed classifications to be made in the future to assist the mapping, management and monitoring of the Australian Marine Jurisdiction.

Acknowledgments

This research was funded by grants number T93/237 and 94/040 from the Fisheries Research and Development Corporation (FRDC). Dr Andrew Forbes and Dr Alan Butler are thanked for review of the manuscript as well as two external reviewers. Our reviewers reminded us that the RoxAnn system and in particular Dr D. Burns has made a valuable contribution to the topic of seabed mapping. We acknowledge this and reinforce it here but point out that users should be cautious when using black box implementations of acoustic backscatter systems without viewing the raw data. Matt Sherlock, Lindsay MacDonald and Jeff Cordell are thanked for assistance in collection of acoustic data at sea. Dr Pavel Sakov and Jason Waring are thanked for the ECHO software developments and assistance in algorithm developments.

References

Barker, B. A. J., Helmond, I., Bax, N. J., Williams, A., Davenport, S., and Wadley, V. A. (1999). A vessel-towed camera platform for surveying seafloor habitats of the continental shelf. *Continental Shelf Research* **19**, 1161–70.

Bax, N., Kloser, R. J., Williams, A., Gowlett-Holmes, K., and Ryan, T. (1999). Seafloor habitat definition for spatial management in fisheries: a case study on the continental shelf of southeast Australia using acoustics and biotic assemblages. *Oceanologica Acta* **22**(6), 705–19.

Bax, N. J., and Williams, A. (Eds.) (2000). Habitat and fisheries productivity in the South East Fishery. Final report to FRDC Project 94/040. (CSIRO Marine Research: Hobart, Australia.)

Bax, N. J., and Williams, A. (2001). Seabed habitat on the south-eastern Australian continental shelf: context, vulnerability and monitoring. *Marine and Freshwater Research* **52**, 491–512.

Chivers, R. C., Emerson, N., and Burns, D. R. (1990). New acoustic processing for underway surveying. *Hydrographic Journal* **56**, 9–17.

Coleman, N., Gason, A. S. H., and Poore, G. C. B. (1997). High species richness in the shallow marine waters of south-east Australia. *Marine Ecology Progress Series* **154**, 17–26.

Collins, W., Gregory, R., and Anderson, J. (1996). A digital approach to seabed classification. Sea Tech, August 83–7. ISSN 0093-3561.

Folk, R. L. (1968). 'Petrology of Sedimentary Rocks.' (Hemphill: Austin, TX.)

Foote, K. G. (1982). Optimizing copper spheres for precision calibration of hydroacoustic equipment. *Journal of the Acoustical Society of America* **71**, 742–7.

Greenstreet S. P. R., Tuck I. D., Grewar G. N., Armstrong E., Reid D. G., and Wright P. J. (1997). An assessment of the acoustic survey technique, RoxAnn, as a means of mapping seabed habitat. *ICES Journal of Marine Science* **54**, 939–59.

Hamilton, L. J., Mulhearn, P. J., and Poeckert, R. (1999). ComparisonHamilton, L. J., Mulhearn, P. J., and Poeckert, R. (1999). Comparison of RoxAnn and QTC-View acoustic bottom classification system performance for the Cairns area, Great Barrier Reef, Australia. *Continental Shelf Research* **19**, 1577–97.

Heald, G. J., and Pace, N. G. (1996). An analysis of the 1st and 2nd backscatter for seabed classification. In 'Proceedings of the 3rd European Conference on Underwater Acoustics, 24–28 June 1996'. Vol. II. (Ed. J. S. Papadakis.) pp. 649–54. (Crete University Press.)

Jackson, D. R., Winebrenner, D. P., and Ishimaru, A. (1986). Application of the composite roughness model to high-frequency bottom scattering. *Journal of the Acoustical Society of America* **79**(5), 1410–22.

Jones, H. A., and Davies, P. J. (1983). Superficial sediments of the Tasmanian continental shelf and part of Bass Strait. Bureau of Mineral Resources, Geology and Geophysics Bulletin No. 218. (Australian Government Publishing Service.) ISBN 0 644 02686 3. 25 pp.

Kaiser, M. J.; Armstrong, P. J.; Dare, P. J., and Flatt, R. P. (1998). Benthic communities associated with a heavily fished scallop ground in the English Channel. *Journal of the Marine Biological Society* **78**(4), 1045–59

Kavli, T., Weyer, E., and Carlin, M. (1994). Real time seabed classification using multi frequency echo sounders. In 'Proceedings of Oceanology International 94, Brighton, UK, March 1994'. Vol. 4, 1–9.

Kloser, R. J., Sakov, P. V., Waring, J. R., Ryan, T. E., and Gordon, S. R. (1998). Development of software for use in multi-frequency acoustic biomass assessments and ecological studies. CSIRO Report to Fisheries Research and Development Corporation T93/237: 74 pp. (CSIRO Marine Research: Hobart, Australia.) ISBN 0 643 06192.4.

Lurton, X., and Pouliquen, E. (1992). Automated seabed classification system for echo-sounders. In 'Oceans 92, Vol. 1'. pp. 317–21. (IEEE: New York.)

Magorrian, B. H., Service, M., and Clarke, W. (1995). An acoustic bottom classification survey of Strangford Lough, Northern Ireland. *Journal of the Marine Biological Association United Kingdom* **75**, 987–92.

Orlowski, A. (1984). Application of multiple echoes energy measurements for evaluation of sea-bed type. *Oceanologia* **19**, 61–78.

Pitcher C. R., Gordon, S. R., Kloser, R. J., and Jones, P. N. (1999). Development of an acoustic system for remote sensing of benthic fisheries habitat for mapping, monitoring and impact assessment. CSIRO Report to Fisheries Research and Development Corporation T93/237: 74 pp. (CSIRO Marine Research: Hobart, Australia.) ISBN 0 643 06196 7.

SIMRAD (1996). Simrad EK500 Scientific Echo Sounder Instruction Manual. Simrad Subsea P2170E. 111 pp. (Simrad: Horton, Norway.)

Snelgrove, P. V. R., and Butman, C. A. (1994). Animal–sediment relationships revisited: cause versus effect. *Oceanography and Marine Biology: an Annual Review* **32**, 111–7.

Urick, R. J. (1983). 'Principles of Underwater Sound.' (McGraw-Hill: New York.) 423 pp.

Waring J. R., Kloser R. J., and Pauly, T. (1994). 'Echo' – managing fisheries acoustic data. In 'Proceedings of the International Conference on Underwater Acoustics. University of New South Wales, December 1994'. pp. 22–4. (Australian Acoustical Society: Darlinghurst Public School, NSW, Australia.)

Manuscript received 10 December 1999; revised and accepted 28 August 2000